ACS Sustainable Chemistry & Engineering

Research Article

pubs.acs.org/journal/ascecg

Valorization of Biorefinery Side-Stream Products: Combination of Humins with Polyfurfuryl Alcohol for Composite Elaboration

Jean-Mathieu Pin,[†] Nathanael Guigo,*[,†] Alice Mija,[†] Luc Vincent,[†] Nicolas Sbirrazzuoli,[†] Jan C. van der Waal,[‡] and Ed de Jong*[,‡]

[†]Université Nice Sophia Antipolis, CNRS, LPMC, UMR 7336, 06100 Nice, France

[‡]Avantium Chemicals B.V., Zekeringstraat 29, 1014 BV Amsterdam, The Netherlands

Supporting Information

ABSTRACT: A challenge of today's industry is to transform low-value side products into more value-added materials. Humins, a byproduct derived from sugar conversion processes, can be transformed into high value-added products. Thermosetting furanic composites were elaborated with cellulose filters. Large quantities of humins were included into a polyfuranic thermosetting network. Comparisons were made with composites generated with polyfurfuryl alcohol (PFA) and with PFA/lignin. It was concluded that new chemical interactions were created between the side-chain oxygen groups of the humins and the PFA network. Analysis of the fracture surface of the composites containing humins lead to the conclusion that higher interfacial bonding and more efficient stress transfer between the matrix and the fibers is present. The higher ductility of the humins-based matrix allows for a two-fold higher tensile strength in comparison with other composites tested. Incorporation of humins decreases the brittleness of the furanic composites, which is one major drawback of the pure PFA composites.

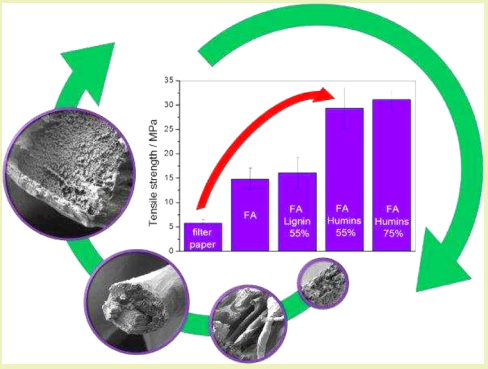

KEYWORDS: *Biorefinery, Humins, Polyfurfuryl alcohol, Composites, Mechanical properties*

INTRODUCTION

The production of new, versatile, carbon-based building blocks from biomass resources is the unique alternative to avert the massive use of petroleum-based chemicals. The conversion of lignocellulosic biomass into fuels and chemicals represents several scientific and technical challenges, covering different fields such as catalysis and chemical engineering.[1,2] For example, 5-hydroxymethylfurfural (HMF) and furfural are two platform chemicals that can be obtained from the dehydration of C_6 and C_5 sugars, respectively, and both can be extracted from the cellulose and hemicellulose fractions. They can be further converted into furanic derivatives such as 2,5-furandicarboxylic acid (FDCA) or furfuryl alcohol (FA), which are well-known precursors to the elaboration of biobased polymers.[3−6]

The growing interest for developing sustainable biomass conversion processes at large scale is exemplified by the Dutch company Avantium, which produces a new class of furanic building blocks called YXY. These furanic molecules have proven to be excellent candidates to design bioplastics and biofuels from first and second generation feedstocks.[4] Avantium has been operating a pilot plant to convert carbohydrates into HMF with a complete capacity of 40 tons/year. To keep the biorefinery operations sound from an environmental and an economical point of view, the pilot plant design and by extension the future biorefinery development need to take into account the valorization of byproducts. Indeed, the conversion of fructose or other C_6 sugars into HMF leads to the formation of black and tarry byproducts which are so-called "humins". Recent studies[7−9] assimilated humins to carbonaceous, heterogeneous, and polydisperse macromolecules, which do not have well-defined structures. They present polyaromatic condensed structures formed by a dehydration pathway containing alcohol, acid, ketone, and aldehyde groups.[8,9] It should also be stressed that humins formation yield and resulting structures strongly depend on the feedstock and processing parameters employed (temperature, pH, reaction time).

Nowadays, humins are mostly considered as a combustible to supply heat and power back into the sugar conversion process. One of the challenges for future biorefinery operations is to transform them into higher value-added products. Hoang et al.[10] for example found new applications for humins such as catalytic gasification to syngas and to hydrogen. This study proposes new application domains for humins and aims to develop for the first time biobased polymeric materials from which substantial parts are made of these recalcitrant byproducts. Van Zandvoort proposed that humins have mainly an aromatic character consisting of essentially furanic moieties.[7]

Received: June 13, 2014
Published: July 17, 2014

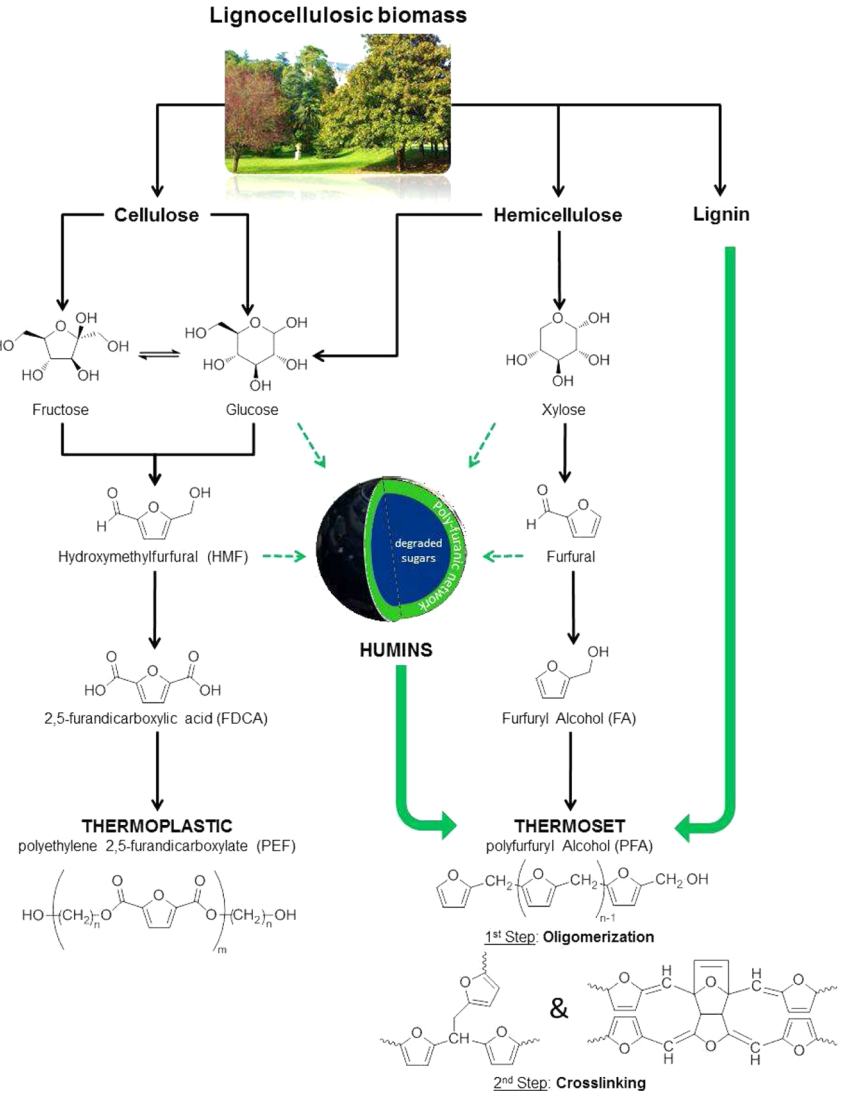

Figure 1. Representative scheme of biorefinery key molecules for furanic-based polymer.

Intrinsically, this would suggest a good compatibility and peculiar chemical affinity with furanic compounds such as furfuryl alcohol. We therefore studied the inclusion of humins as macro-monomers into a polyfurfuryl alcohol network as a good strategy to generate homogeneous and efficient materials. In this case, humins addition on polyfuranic formulation can also reduce the resin cost price. The furfuryl alcohol (FA) is indirectly issued from lignocellulosic biomass conversion via hydrogenation of furfural, and its production has largely increased in the past 20 years.[11] As depicted in Figure 1, this furfural derivative has a high tendency to polymerize under acidic conditions leading to polyfurfuryl alcohol (PFA). This polymerization proceeds via a complex mechanism that can be mostly discriminated in two steps.[12,13] The first one corresponds to acid-induced polycondensation leading to the formation of linear furanic oligomers. Then, tridimensional amorphous networks are generated subsequently by cross-linking both via Mickael addition and Diels–Alder cyclo-additions.[14,15] Indeed the phenomenon of reticulation includes an important transition of the physical state of the reaction medium: from a liquid to a viscoelastic solid.[16]

The PFA-biobased thermosetting resin is largely used in some applications such as foundry resins and composites and also for wood adhesives[17] and impregnation, in particular, with its strong efficiency in terms of biological degradation resistance.[18] The major drawback of the PFA network is its high brittleness, so modification of thermomechanical properties are important issues that need to be addressed. Combination with biobased compounds modifies advantageously the PFA thermomechanical behavior such as introduction of triglyceride flexible moieties.[19] Moreover, it has been proven that the PFA can interact with heterogeneous macromolecular compounds such as tannin[20] or lignin,[21,22] which are also well-known biorefinery byproducts.[23]

According to the above-mentioned features, polyfurfuryl alcohol (PFA) was logically chosen for being combined with humins for three main reasons: (i) The PFA is a biobased polyfuranic, so combination with humins leads to fully biobased furanic resins. (ii) The PFA network develops under acid-induced polycondensation, which is also one the postulated routes for the humins growth.[8,9] (iii) Regarding composite applications, introduction of humins into the dense cross-linked PFA network could modify the thermomechanical properties. The first aim of this work was to prepare stable and homogeneous PFA/humins thermoset resins. Rheological measurements have been conducted to control as much as

dx.doi.org/10.1021/sc5003769 | ACS Sustainable Chem. Eng. 2014, 2, 2182–2190

Table 1. Conditions of Two-Step Precuring

initial w/w ratios: FA/humins/MA, FA/lignin/MA	first precuring step	second precuring step	final resin viscosity at 25 °C (Pa s)	final resin viscosity at 50 °C (Pa s)
95/0/5	40 min at 110 °C	80 °C for 5 min	515	13
40/55H/5	30 min at 120 °C and 30 min at 130 °C	80 °C for 5 min	627	28
40/55L/5	–	80 °C for 5 min	3900	530
20/75H/5	30 min at 120 °C	80 °C for 5 min	2240	59

possible the resin viscosities in order to have comparative samples. Infrared spectroscopy was performed to get structural information on the resins and to highlight potential interactions between the growing PFA network and the humins. As a simple proof-of-concept, thermosetting furanic composites were elaborated with cellulose filters as reinforcement. The mechanical properties of the composites such as stiffness and strength were determined by tensile tests. To further discuss the influence of humins on mechanical properties, comparisons were made with cellulose composite generated with PFA, PFA/humins resin, and PFA/lignin combined resins. Scanning electron microscopy (SEM) of the fracture surface was done to evaluate qualitatively the interface between cellulose fibers and the different matrices.

EXPERIMENTAL SECTION

Materials. Furfuryl alcohol (FA) (purity: ≥ 98%) as monomer and maleic anhydride (MA) (purity: ≥ 99%) as polymerization catalyst were purchased from Sigma-Aldrich and were used as received.

Humins are directly produced by Avantium Chemicals at their Pilot Plant in Geleen, The Netherlands, by conversion of fructose in methanol solvent. These humins were distilled under high vacuum to reach low 5-hydroxymethylfurfural (HMF) and 5-methoxymethylfurfural (MMF) content (<5% by weight). The humins composition obtained by elemental analysis is approximately of 60 wt % C, 32 wt % O, and 5 wt % H being in good correlation with other reported values.[7,10] Their heating value is around 23 MJ/kg. Humins have the appearance of a very viscous, shiny, black bitumen.

Organosolv lignin was provided by ECN.[4] A precise description of this lignin can be found in the de Wild et al. paper.[24] The brown solid was finely crushed and passed through a sieve in order to have a good dispersion in the FA monomer.

PFA/humins/cellulose and also PFA/lignin/cellulose composites were made with Whatman 40 filter paper having a diameter of 110 mm and a weight of 900 mg.

Resins and Composites Preparation. Resin formulations were designed in order to reach approximately the same viscosity for each sample so to achieve similar impregnation conditions. The weight ratio of the different formulations, procedures of resinification, and final viscosities of each resin are summarized in Table 1. Note that it was necessary to adapt the precuring time and temperatures for each composition due to their different reactivity and viscosity. Four formulations were prepared.

The reference PFA resin consisted of 95% of FA and 5% of MA on weight basis. This quantity of catalyst was chosen as the optimal concentration, considering that probable interaction between MA and humins will consume MA and thus decrease the intrinsic FA reactivity. This assumption was confirmed by DSC studies performed with the classical catalyst amount, i.e., 2% of MA (Supporting Information).[16] As shown in Table 1, the acidic catalyst (MA) was added in two steps to allow formation of a homogeneous viscous PFA resin and to reach a higher precuring temperature in the first step, followed by cooling the mixture to 80 °C to proceed with the second addition of 2.5% of MA. This two-step procedure was used because it would otherwise be difficult to have a good control of the reaction temperature, with FA polymerization being a very exothermic reaction. Indeed, the resinification was much more difficult to control when the catalyst was added in one single step. This reference resin is reported as 95/0/5.

Two formulations containing humins were prepared. FA/humins/MA weight ratios were respectively 40/55H/5 and 20/75H/5 (Table 1). Prior to the addition of the acidic initiator, FA (either 40 or 20% w/w) was mixed with humins (either 55 or 75% w/w) at 105 °C for 20 min under mechanical stirring until a homogeneous, viscous, black liquid was formed. Then, the maleic anhydride (5% w/w) was introduced in two equal steps of 2.5% w/w MA. On the basis of DSC investigations (not shown here), introduction of viscous condensed humins into the system decreases the overall reactivity and shifts the polycondensation peak to a higher temperature compared to those of the pure FA/MA mixtures. The first precuring steps were performed slightly longer and at a higher temperature range in the presence of humins (Table 1). After cooling to 80 °C, the last addition of 2.5% w/w MA was done. Subsequently, the mixture was stirred for another 5 min and cooled to room temperature. A homogeneous, viscous, shiny, black resin was obtained in each case. The resins were stored in the fridge, and no phase separation was observed after several weeks.

A resin was also prepared with an organosolv lignin. The FA/lignin/MA weight ratio was 40/55L/5. First, FA was mixed with 55% of the organosolv lignin and heated to 105 °C for 20 min under mechanical stirring. Then the mixture was cooled to 80 °C, and 5% of MA was added. In this case, MA was introduced in one single step. Otherwise, the viscosity, which is already very high due to introduction of the lignin powder, rose rapidly during the prepolymerization (Table 1).

Fiber Composites Preparation. Cellulose filter papers were impregnated with the different above-mentioned thermosetting resins in order to achieve a 1:1 weight ratio between cellulose reinforcement and the cured thermosetting resin. In each case, the resin was spread homogeneously on the surface of cellulose filter. Then, these impregnated filters were protected by two sheets of kapton films and placed between two aluminum blocks to ensure uniform repartition of the resin during the curing. The system was placed in a ventilated oven and was cured at 160 °C during 3 h. This curing protocol was elaborated in good agreement with DSC investigation (Supporting Information) to reach a maximal conversion.

EXPERIMENTAL TECHNIQUES

Rheometry. An Anton Paar MCR 102 rheometer was used to measure the resin viscosities in shear mode (0.1 to 10 Hz) with parallel plate−plate geometries (15 mm diameter and 1 mm gap).

Infrared Spectroscopy. FTIR was employed to analyze the structural evolution of the resin after the precuring step and to highlight potential covalent bonds between humins and FA matrix. For this purpose, furfuryl alcohol, the 95/0/5 and 40/55H/5 resins, and the completely cured 40/55H/5 thermoset spectra were recorded. All resin formulations were prepared according to the Table 1 recipe. A PerkinElmer Spectrum BX II spectrophotometer was used in attenuated total reflectance (ATR) mode with a diamond crystal. The spectrum of air was recorded as background. A total of 1000 scans with a resolution of 1 cm^{-1} was recorded for each sample to obtain sufficient sensivity.

Scanning Electron Microscopy (SEM). The morphologies of cellulose composite strips after tensile test fracture were investigated by scanning electron microscopy (SEM) at the Microscopy Centre of University Nice Sophia Antipolis using a JEOL 6700F microscope equipped with a field emission gun. The electron beam voltage was

fixed to 1 kV. The samples were mounted on the microscope studs using silver colloidal paste and sputter coated with gold palladium.

Tensile Tests. The stress−strain curves were recorded on an Instron 5565 apparatus in tensile mode with crosshead speed of 2 mm min^{-1}. After curing, the impregnated cellulose filters were cut into strips of around 100 × 10 × 0.25 (length × width × thickness) mm. The length between the clamps was fixed to 80 mm. For each composite, the average values and standard deviations of Young's modulus and tensile strength were calculated from seven measurements.

RESULTS AND DISCUSSIONS

FT-IR Analysis of PFA/Humins Thermoset Resins. The ATR-IR spectra of the neat FA monomer and the raw humins are shown in Figure 2 together with the spectra of the 95/0/5 resins and the 40/55H/5 resins. The assignment of major bands, in good agreement with the literature,[25,26] is also summarized in Table 2. At first look, the four spectra do not exhibit major differences, which would indicate that similar functional groups are present in the different systems under study.

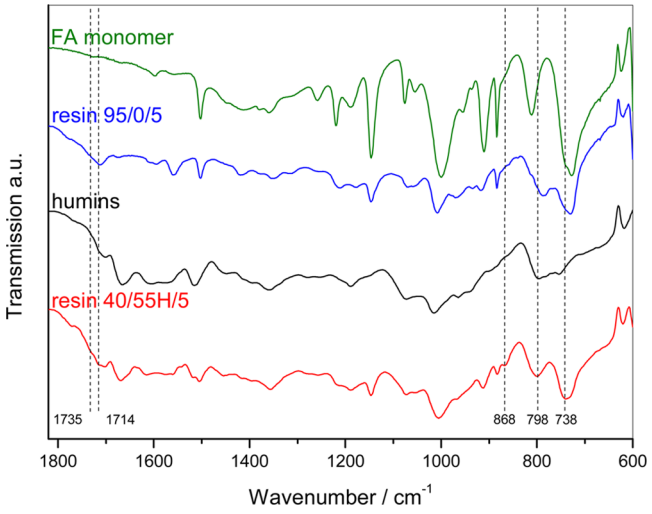

Figure 2. IR spectra of FA monomer (green), humins (black), precured resins 95/0/5 (blue), and 40/55H/5 (red).

The spectrum of the FA monomer contains many peaks that can be assigned to vibrations respectively associated with the furan ring or the hydroxymethyl group.[25] The furan C=C stretching vibration appears at 1505 cm^{-1}, while the peaks around 812 and 728 cm^{-1} can be assigned to the C−H out-of-plane deformation of the furan ring (Figure 2). The strong peak around 1000 cm^{-1} corresponds to the C−O stretching of the hydroxymethyl group. The strong peak at 1146 cm^{-1} is commonly attributed to the C−O stretching of the furan ring collectively associated with C−H and OH wagging.[25,26] Thus, this peak associates with two other FA characteristic peaks at 1220 and 884 cm^{-1} (assigned in Table 2) can be an indication of the free FA in the precured resin composition. Indeed, this peak is also visible in 95/0/5 and 40/55H/5 in quite the same intensity, which means the precured step has been conducted approximately in the same conditions.

When FA is prepolymerized into PFA, new bands are developing while others are shifting. As shown in Figure 2, the spectrum of 95/0/5 shows a new peak at 1559 cm^{-1}, which is assigned to C=C stretching in a 2,5-disubstituted furan ring. The red-shift of the C−H out-of-plane deformation from 812 to around 790 cm^{-1} is taken as another proof of the furan substitution in the C_5 position. Moreover, the appearance of a composite peak between 1720 and 1690 cm^{-1} indicates that carbonyl moieties could have been created through hydrolytic opening reactions of the furan ring. These peaks could also correspond to Diels−Alder cycloadducts, which are thought to be formed during PFA cross-linking.[14] All the above-mentioned features are consistent with previous IR studies on FA polymerization.[16,26,27]

Table 2. Assignment of Major Bands on FT-IR Spectra

assignment	wavenumber (cm^{-1})	in spectrum of
C−H wagging furan ring	728	FA
C−H wagging furan ring	738	40/55H/5
C−H wagging 5-sub furan ring	790	95/0/5
C−H wagging furan ring	798	40/55H/5
C−H wagging furan ring	812	FA
C−H wagging methylene group/C−O stretching D−A adduct	868	40/55H/5
C−C−C in-plane bending furan ring	886	FA
C−O stretching hydroxymethyl group	1000	FA
C−O stretching	1020	humins
C−O stretching furan ring and met C−H wagging and OH wagging	1146	FA
C−C/C-O stretching furan ring/C−C stretching hydroxymethyl group	1220	FA
C=C stretching furan ring	1505	FA
C=C stretching HMF's furan ring	1515	humins
C=C stretching 2,5-subfuran ring	1559	95/0/5
C=C stretching conjugated with C=O	1600	humins
C=O stretching MMF/HMF's aldehyde	1665	humins
C=O stretching	1690	95/0/5
C=O stretching conjugated with C=C	1712	humins
C=O stretching	1714	40/55H/5
C=O stretching	1720	95/0/5
C=O stretching	1735	40/55H/5

dx.doi.org/10.1021/sc5003769 | ACS Sustainable Chem. Eng. 2014, 2, 2182−2190

The fructose-based humins spectrum shown in Figure 2 is consistent with previous FT-IR studies conducted on such complex polyaromatic structures.[7−9] The molecular structure of humins is mainly derived from HMF and 5-methoxymethylfurfural (MMF). The peak at 1515 cm^{-1} is assigned to C=C stretching in furan rings, while the peak at 1020 correspond to C−O stretching. As for PFA, the composite peaks between 800 and 750 cm^{-1} are attributed to the out-of-plan C−H bending of the different substituted furans. According to Lund et al., the peak at 1712 cm^{-1} together with the peak around 1600 cm^{-1} in humins are characteristic of carbonyl group conjugated to an alkene group. Finally, it should be mentioned that the feature at 1665 cm^{-1} could arises from the C=O stretch of the MMF's and HMF's aldehyde group.[8]

The spectrum of the prepolymerized 40/55H/5 resin corresponds approximately to the superposition of the signals from the 95/0/5 PFA resin and those from the humins. However, some features can be attributed to specific interactions between the PFA network and the humins. A new band develops at 868 cm^{-1}, which is neither visible in the spectrum of PFA resin or in the spectrum of humins. The peaks appearing within this wavenumber region are generally attributed either to C−H wagging of methylene linkages or C−O stretching from Diels−Alder cycloadducts.[26] This might indicate that novel kinds of interactions were created between the side-chain oxygen groups of the humins and the furanic rings from the PFA. Moreover, clear-cut shoulders appear at 1714 and 1735 cm^{-1} in the carbonyl stretching region. The chemical environment of the carbonyl groups present in the aliphatic parts of the humins has been modified probably due to new interactions with the polyfurfuryl alcohol network. It should also be mentioned that the C−H out-of-plane bending of the furan rings appears at 798 and 738 cm^{-1} for the 40/55H/5 resin. These peaks are broader and slightly shifted to higher wavenumbers compared to the PFA resin. It denotes a more complex network of furan rings due to interconnections between the two systems. A putative chemical structure of the humins surface based on the literature[7,9] and FTIR measurements is proposed in Figure 3 to highlight its possible covalent interactions with FA oligomers.

Mechanical Properties. *Effect of Humins Amount on PFA Blend.* Figure 4 shows the stress−strain curves of the nonimpregnated cellulose paper together with those of the different cellulose/thermosets composites. The curve of the cellulose paper reveals a succession of fractures that can be attributed to the progressive disentanglement of the fibers during the tensile test.[28] As observed on the SEM micrographs (Figure 4E), the fracture surface of the cellulose paper confirms the loosening of fibers. In comparison, the stress−strain behavior of the thermoset composites impregnated cellulose fibers are very different and can be characterized in first approximation to a straight line for the tensile strength that is characteristic of an elastic response, leading to a brittle fracture. Such behavior reveals an uniform impregnation leading with an adhesion between the cellulose fibers and the matrix. These results are corroborated with the SEM micrographs presented in Figure 4. Compared to the cellulose filter, the impregnated composites present a sharper fracture surface.

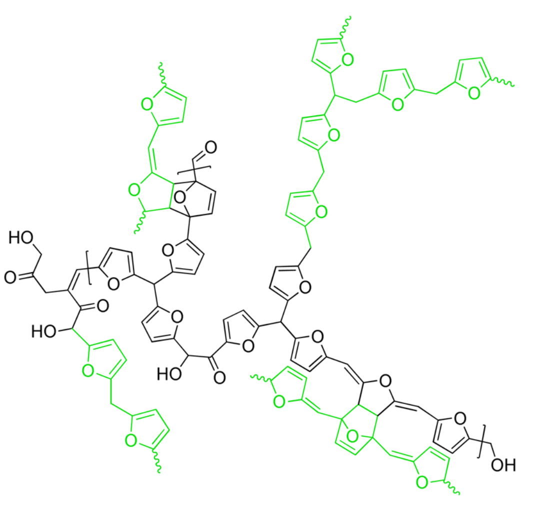

Figure 3. Putative cross-links between humins structures taken from the literature (black) and FA oligomers (green).[7,9]

The Young modulus and tensile strength at failure obtained for the different composites are gathered in Figure 5. As all the cellulose filters have similar mechanical behavior, the differences in the mechanical responses of the composites are only linked to the matrix and its abilities to generate good adhesivity with the fiber reinforcement. When the PFA resin is used, the resulting composite exhibits a Young modulus of about 3.5 GPa. The tensile strength approaches 15 MPa, while the strain at failure does not exceed 0.5% (Figure 4). This denotes an extremely brittle behavior generated by the PFA network, which is characteristic for this peculiar thermosetting resin.[29] As shown in Figures 4 and 5, the incorporation of organosolv lignin within the PFA matrix does not dramatically change the mechanical properties of the composite. Similar tensile modulus and strength compared to the PFA resin indicates that organosolv lignin does not modify the brittleness of the composite and interfacial adhesion between the furanic matrix and cellulose fibers. Like the PFA resin, the lignin also exhibits a rigid aromatic structure that is not able to sufficiently flexibilize the cross-linked network.

On the other hand, the incorporation of humins into the matrix leads to a significant improvement of the composite mechanical properties. When the 40/55H/5 resin is used as matrix, the Young modulus reaches ∼4 GPa, and the tensile strength (∼28 MPa) increases by a factor of two compared to those of the PFA-based composite. Such behavior could result from better stress transfer between the matrix and the cellulose fibers. Moreover, the incorporation of humins unambiguously changes the mechanical behavior of the matrix itself, which is likely to become more ductile and flexible compared to the rigid PFA network. This is particularly reflected in Figure 4, which highlights a plastic contribution on the stress−strain curve when the amount of humins in the matrix increases to 75% w/w. Consequently, the composite prepared with the 20/75H/5 resin has a tensile modulus of about 3 GPa, which is lower compared to the other composites. However, it should be outlined here that the tensile strength of the 20/75H/5 composite reaches ∼32 MPa, which is significantly higher compared the values obtained with the PFA and the PFA/lignin resins. The higher ductility of the humins-based matrix allow it to reach a higher level of strength without sacrificing interfacial bonding with the cellulose fibers. The humins micro-architecture can be schematically considered as a core−shell rubber. Several studies have demonstrated that the humins surface presents a rigid aromatic structure, while the ductile core is mostly constituted by nonaromatic moieties derived from degraded sugar.[30,31] Then, the incorporation of humins

dx.doi.org/10.1021/sc5003769 | ACS Sustainable Chem. Eng. 2014, 2, 2182−2190

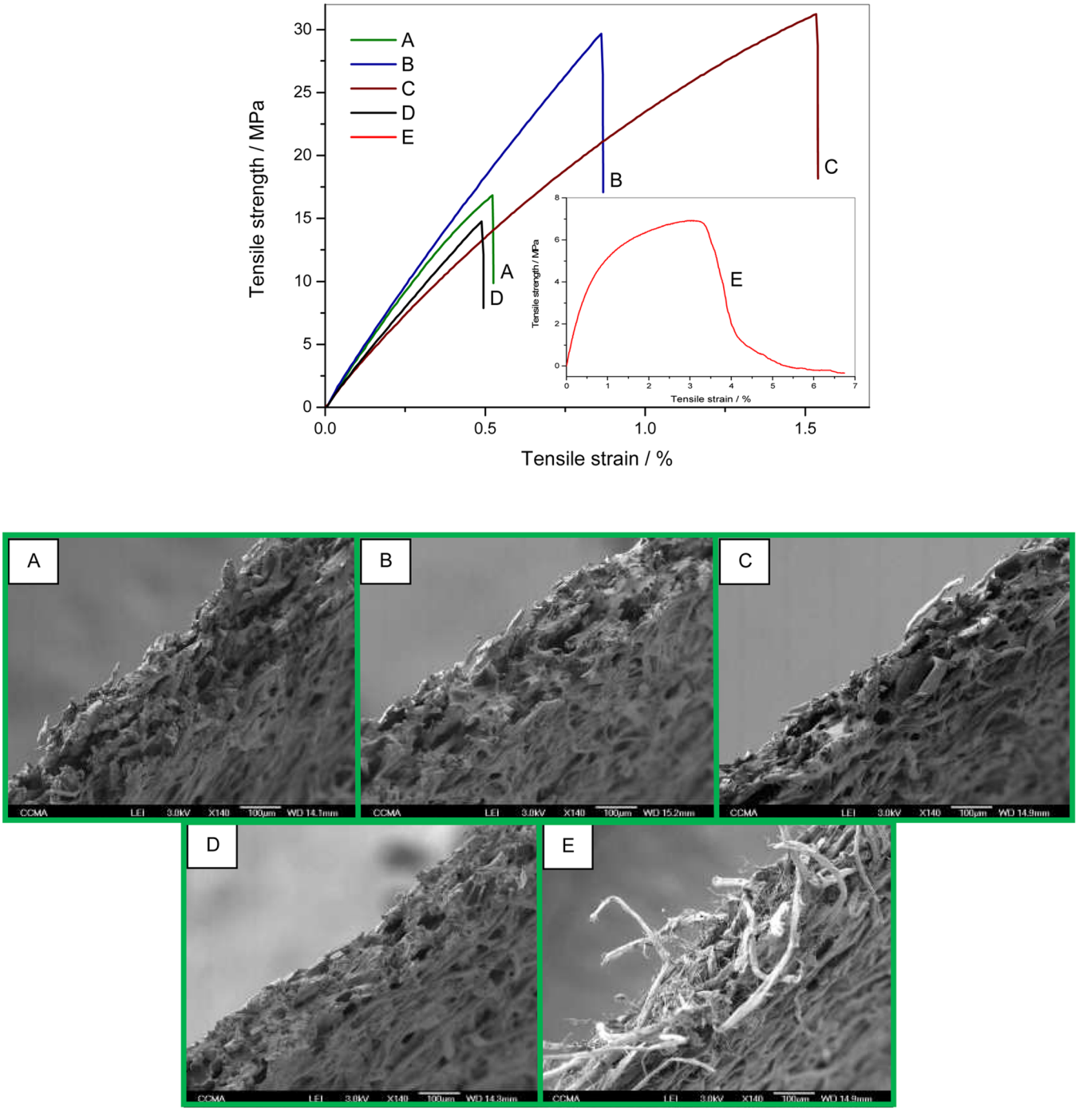

Figure 4. Stress–strain curves and SEM fracture surface: (A) 40/55L/5, (B) 40/55H/5, (C) 20/75H/5, (D) 95/0/5, and (E) filter paper.

into the PFA matrix will induce higher flexibility. Such behavior is also observed when core–shell rubber microparticles are incorporated into a brittle matrix.[32,33]

Morphology of Composites. The SEM micrographs shown in Figure 6 exhibit the fracture surface of the different composites. Each picture reveals, in good agreement with the stress–strain curves, a homogeneous resin impregnation that partly fills the empty spaces present between the cellulosic fibers of the filter paper. The fracture surface of the PFA composite (Figure 6D) highlights fibers that are embedded within the matrix but do not show fiber fracture or dislocation. The fracture seems to originate from the matrix itself. It corroborates the tensile measurements, which denote the brittle behavior of the composite. The presence of scattered resin fragments at the surface of the PFA/lignin-based composite (Figure 6A) also confirms the brittleness of this type of resin. The matrix appears in the form of fragmented and brittle mortar. A pulled-out single fiber can be clearly seen, which would be the consequence of moderate interfacial bonding between the PFA/lignin matrix and the cellulosic fibers.

Interestingly, the fracture surface of the composites containing humins in the matrix reveals more fiber dislocation or rupture (Figure 6B and C). It would attest for higher interfacial bonding and more efficient stress transfer between the matrix and the fibers. Moreover, the matrix appears more ductile with fewer striations compared to the neat PFA and the

dx.doi.org/10.1021/sc5003769 | ACS Sustainable Chem. Eng. 2014, 2, 2182–2190

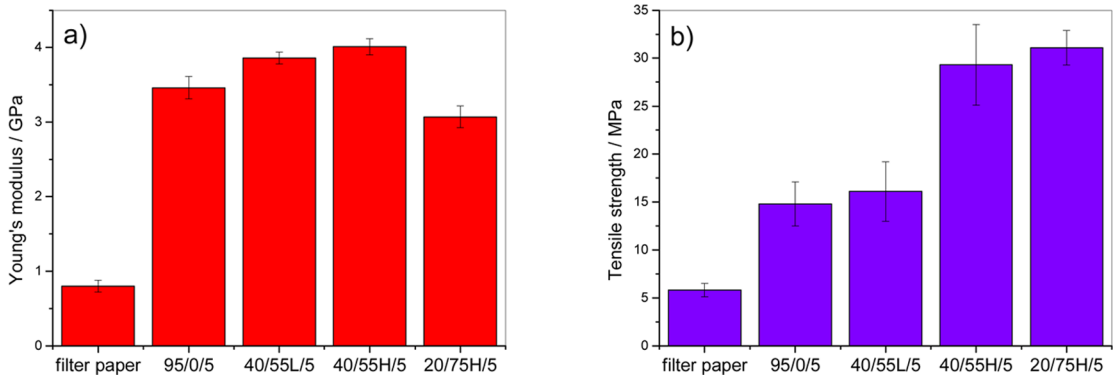

Figure 5. Young's modulus (a) and tensile strength (b) histograms.

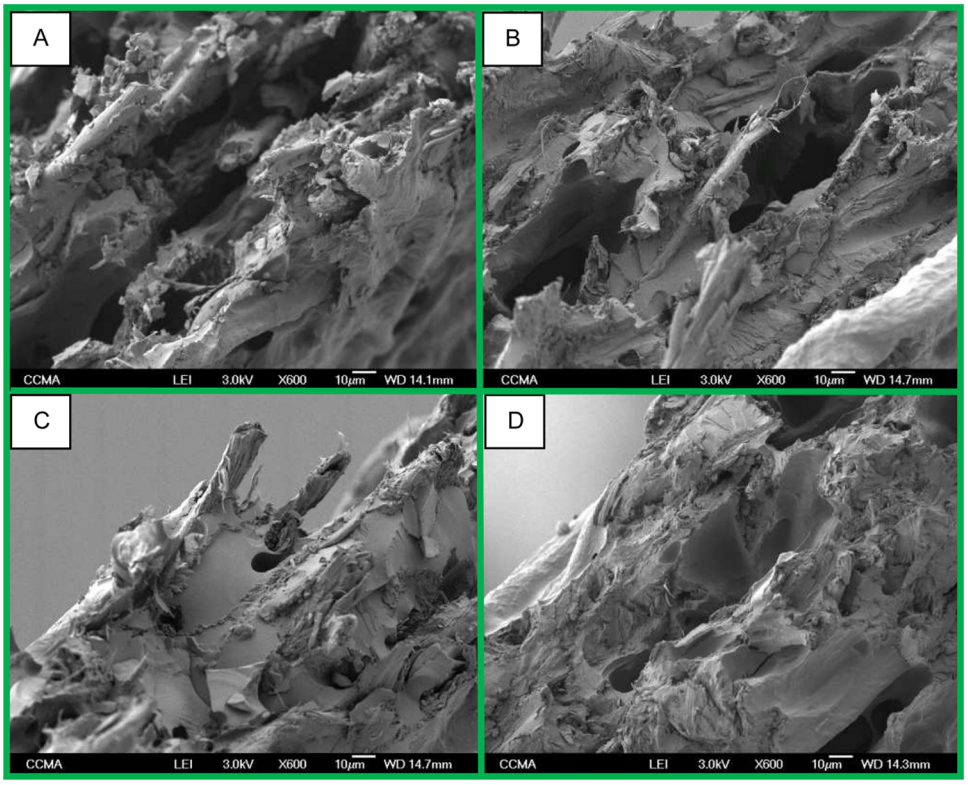

Figure 6. SEM micrographs on fracture composites after tensile test (×600): (A) 40/55L/5, (B) 40/55H/5, (C) 20/75H/5, and (D) 95/0/5.

PFA/lignin resins. These observations correlate well with the higher tensile strength obtained for the PFA/humins-based composites. The images in Figure 7 are obtained for the composite processed with the 40/55H/5 based-resin and focus on the fiber/matrix interface. At higher magnitude, the formation of a homogeneous resin coating is distinctly highlighted at the surface of the fiber. No voids or cracks are observed, indicating good interfacial bonding. These observations confirm that humins play a positive role on the resin ductility and on the cellulose/matrix interface. These additional features underline the great potential for use of humins as raw components into the PFA resins.

CONCLUSIONS

This study has shown that large quantities of humins (either 55 or 75% w/w) can be successfully included into a polyfuranic thermosetting network, which is a good solution to obtain lower cost price resins. Homogeneous systems comprising polyfurfuryl alcohol (PFA) and humins have been prepared via acid-induced polymerizations. FT-IR measurements have shown that potential interactions have been developed between the PFA and the humins network. The PFA/humins resins exhibit reasonably low viscosities for being impregnated onto cellulose filter and lead to cross-linked composites after final curing. The tensile strength of the PFA/humins-based composites is two times higher than those obtained either with the neat PFA composites or the PFA/lignin composites. Incorporation of humins allows for a decrease in the brittleness of the furanic matrix and an increase in the interfacial bonding with cellulose fibers. In agreement with the tensile test data, the SEM observations reveal that the PFA/humins composites present more fiber fractures than the other composites. It confirms that incorporation of humins impacts positively the mechanical properties of the thermosetting composites. This study demonstrates that humins can be valorized as an active component into PFA and in the meantime decreases its

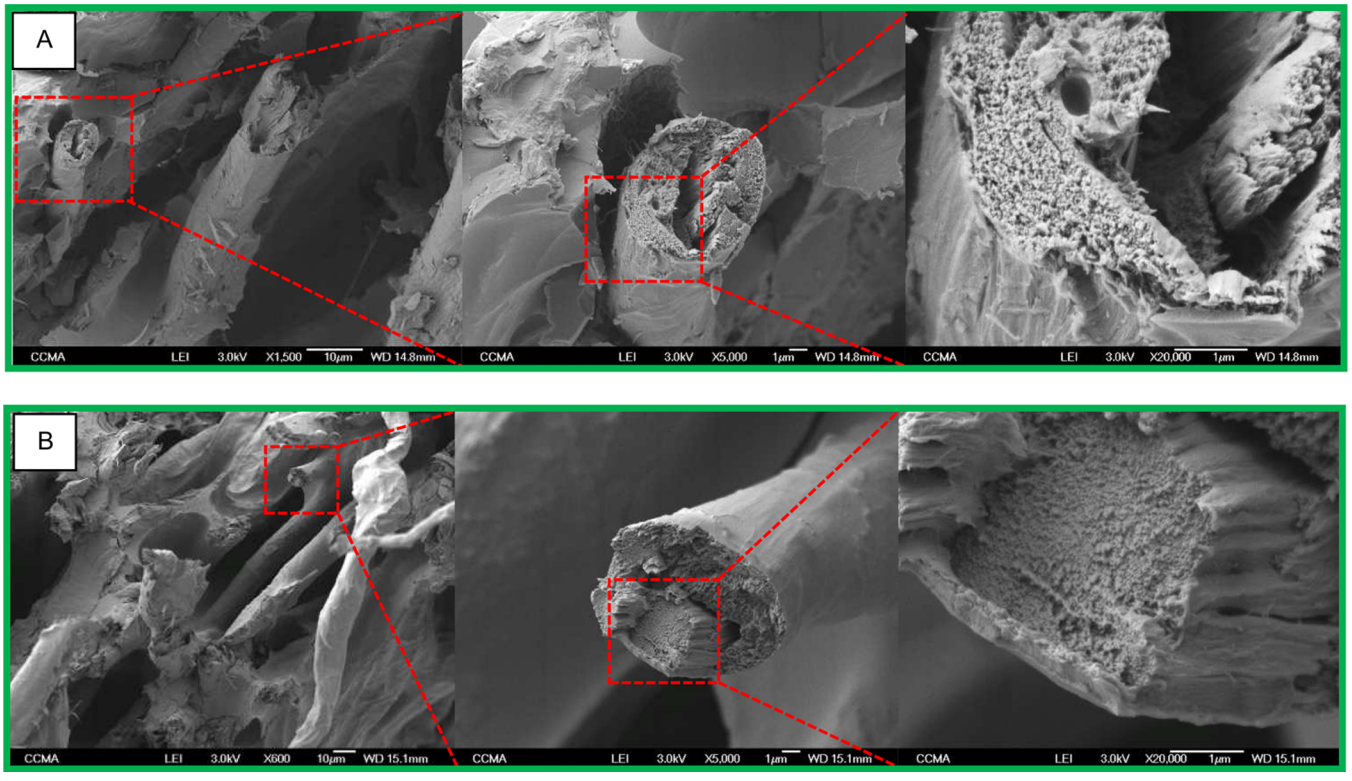

Figure 7. SEM micrographs focused on fiber/matrix interfaces on PFA/lignin (A) or PFA/humins (B) composites.

brittleness, which is one major drawback of the pure polyfurfuryl alcohol biobased thermoset. As proof-of-concept, this precursory work opens gates to further develop reactive humins-based resins both for wood adhesion (plywood, fiberboards) and for wood durability. Further works are currently ongoing to highlight the influence of humins on FA polymerization and on the thermo-mechanical properties of the resulting bulk.

■ ASSOCIATED CONTENT

Ⓢ Supporting Information

Data information about the reactivity of FA/humins formulations with MA is provided by DSC measurements. This material is available free of charge via the Internet at http://pubs.acs.org.

■ AUTHOR INFORMATION

Corresponding Authors

*E-mail: guigo@unice.fr (N. Guigo).
*E-mail: ed.dejong@avantium.com (E. de Jong).

Notes

The authors declare no competing financial interest.

■ ACKNOWLEDGMENTS

The authors acknowledge the European Commission for financial support: BIOFUR FP7-PEOPLE-2012-IAPP project "BIOpolymers and BIOfuels from FURan based building blocks". Also, special thanks to M. Jean-Pierre Laugier for his help and assistance with SEM observations performed at CCMA Common Center of Applied Electronic Microscopy of University of Nice Sophia Antipolis.

■ REFERENCES

(1) Binder, J. B.; Raines, R. T. Simple chemical transformation of lignocellulosic biomass into furans for fuels and chemicals. *J. Am. Chem. Soc.* **2009**, *131*, 1979−1985.
(2) Chheda, J. N.; Huber, G. W.; Dumesic, J. A. Liquid-phase catalytic processing of biomass-derived oxygenated hydrocarbons to fuels and chemicals. *Angew. Chem., Int. Ed.* **2007**, *46*, 7164−7183.
(3) van Putten, R.-J.; van der Waal, J. C.; de Jong, E.; Rasrendra, C. B.; Heeres, H. J.; de Vries, J. G. Hydroxymethylfurfural, a versatile platform chemical made from renewable resources. *Chem. Rev.* **2013**, *113*, 1499−1597.
(4) Eerhart, A. J. J. E.; Huijgen, W. J. J.; Grisel, R. J. H.; van der Waal, J. C.; de Jong, E.; de Sousa Dias, A.; Faaij, A. P. C.; Patel, M. K. Fuels and plastics from lignocellulosic biomass via the furan pathway; a technical analysis. *RSC Adv.* **2014**, *4*, 3536−3549.
(5) Werpy, T.; Petersen, G. *Top Value Added Chemicals from Biomass*; U.S. Department of Energy: Oak Ridge, TN, 2004.
(6) Bozell, J. J.; Petersen, G. R. Technology development for the production of biobased products from biorefinery carbohydrates—The US Department of Energy's "Top 10" revisited. *Green Chem.* **2010**, *12*, 539−554.
(7) van Zandvoort, I.; Wang, Y.; Rasrendra, C. B.; van Eck, E. R. H.; Bruijnincx, P. C. A.; Heeres, H. J.; Weckhuysen, B. M. Formation, molecular structure, and morphology of humins in biomass conversion: influence of feedstock and Processing Conditions. *ChemSusChem* **2013**, *6*, 1745−1758.
(8) Patil, S. K. R.; Lund, C. R. F. Formation and growth of humins via aldol addition and condensation during acid-catalyzed conversion of 5-hydroxymethylfurfural. *Energy Fuels* **2011**, *25*, 4745−4755.
(9) Patil, S. K. R.; Heltzel, J.; Lund, C. R. F. Comparison of structural features of humins formed catalytically from glucose, fructose, and 5-hydroxymethylfurfuraldehyde. *Energy Fuels* **2012**, *26*, 5281−5293.
(10) Hoang, T. M. C.; Lefferts, L.; Seshan, K. Valorization of humin-based byproducts from biomass processing−A route to sustainable hydrogen. *ChemSusChem* **2013**, *6*, 1651−1658.

(11) Hoydonckx, H. E.; van Rhijn, W. M.; Van Rhijn, W.; De Vos, D. E.; Jacobs, P. A. Furfural and Derivitives. In *Ullmann's Encyclopedia of Industrial Chemistry*; Wiley-VCH: Weinheim, Germany, 2007; p 1−29.
(12) Milkovic, J.; Myers, G. E.; Young, R. A. Interpretation of curing mechanism of furfuryl alcohol resins. *Cellul. Chem. Technol.* **1979**, *13*, 651−72.
(13) Gandini, A.; Belgacem, N. M. Furans in polymer chemistry. *Prog. Polym. Sci.* **1997**, *22*, 1203−1379.
(14) Choura, M.; Belgacem, N. M.; Gandini, A. Acid-catalyzed polycondensation of furfuryl alcohol: Mechanisms of chromophore formation and cross-linking. *Macromolecules* **1996**, *29*, 3839−3850.
(15) Montero, A. L.; Montero, L. A.; Martínez, R.; Spange, S. *Ab initio* modelling of crosslinking in polymers. A case of chains with furan rings. *J. Mol. Struct.: THEOCHEM* **2006**, *770*, 99−106.
(16) Guigo, N.; Mija, A.; Vincent, L.; Sbirrazzuoli, N. Chemo-rheological analysis and model-free kinetics of acid catalyzed furfuryl alcohol polymerization. *Phys. Chem. Chem. Phys.* **2007**, *9*, 5359−5366.
(17) Belgacem, N. M.; Gandini, A. Furan-based adhesives. In *Handbook of Adhesive Technology*; Belgacem, N. M.; Gandini, A., Eds.; Marcel Dekker, Inc.: New York, 2003; Chapter 30.
(18) Lande, S.; Westin, M.; Schneider, M. Properties of furfurylated wood. *Scand. J. For. Res.* **2004**, *6*, 22−30.
(19) Gandini, A. Polymers from renewable resources: A challenge for the future of macromolecular materials. *Macromolecules* **2008**, *41*, 9491−9504.
(20) Li, X.; Nicollin, A.; Pizzi, A.; Zhou, X.; Saugeta, A.; Delmotte, L. Natural tannin−furanic thermosetting moulding plastics. *RSC Adv.* **2013**, *3*, 17732−17740.
(21) Guigo, N.; Mija, A.; Vincent, L.; Sbirrazzuoli, N. Eco-friendly composite resins based on renewable biomass resources: polyfurfuryl alcohol/lignin thermosets. *Eur. Polym. J.* **2010**, *46*, 1016−1023.
(22) Nordstierna, L.; Lande, S.; Westin, M.; Karlsson, O.; Furó, I. Towards novel wood-based materials: chemical bonds between lignin-like model molecules and poly(furfuryl alcohol) studied by NMR. *Holzforschung* **2008**, *62*, 709−713.
(23) Thakur, V. K.; Thakur, M. K.; Raghavan, P.; Kessler, M. R. Progress in green polymer composites from lignin for multifunctional applications: A review. *ACS Sustainable Chem. Eng.* **2014**, *2*, 1072−1092.
(24) de Wild, P. J.; Huijgen, W. J. J.; Heeres, H. J. Pyrolysis of wheat straw-derived organosolv lignin. *J. Anal. Appl. Pyrolysis* **2012**, *93*, 95−103.
(25) Barsberg, S.; Berg, R. W. Combined Raman spectroscopic and theoretical investigation of fundamental vibrational bands of furfuryl alcohol (2-furanmethanol). *J. Phys. Chem. A* **2006**, *110*, 9500−9504.
(26) Barsberg, S.; Thygesen, L. G. Poly(furfuryl alcohol) formation in neat furfuryl alcohol and in cymene studied by ATR-IR spectroscopy and density functional theory (B3LYP) prediction of vibrational bands. *Vib. Spectrosc.* **2009**, *49*, 52−63.
(27) Conley, R. T.; Metil, I. An investigation of the structure of furfuryl alcohol polycondensates with infrared spectroscopy. *J. Appl. Polym. Sci.* **1963**, *7*, 37−52.
(28) Nishino, T.; Arimoto, N. All-cellulose composite prepared by selective dissolving of fiber surface. *Biomacromolecules* **2007**, *8*, 2712−2716.
(29) Lawrence, A.; Pranger, G. A.; Nunnery, R. T. Mechanism of the nanoparticle-catalyzed polymerization of furfuryl alcohol and the thermal and mechanical properties of the resulting nanocomposites. *Composites, Part B* **2012**, *43*, 1139−1146.
(30) Sevilla, M.; Fuertes, A. B. The production of carbon materials by hydrothermal carbonization of cellulose. *Carbon* **2009**, *47*, 2281−2289.
(31) Sevilla, M.; Fuertes, A. B. Chemical and structural properties of carbonaceous products obtained by hydrothermal carbonization of saccharides. *Chem.−Eur. J.* **2009**, *15*, 4195−4203.
(32) Pearson, R. A.; Yee, A. F. Influence of particle size and particle size distribution on toughening mechanisms in rubber-modified epoxies. *J. Mater. Sci.* **1991**, *26*, 3828−3844.
(33) Giannakopoulos, G.; Masania, K.; Taylor, A. C. Toughening of epoxy using core−shell particles. *J. Mater. Sci.* **2011**, *46*, 327−338.